PHYSICAL REVIEW B **66**, 140401(R) (2002)

Magnetic circular dichroism in $2p3p3p$ resonant photoemission from ferromagnetic Ni in perpendicular geometry across the L_3 edge

M. Taguchi and G. van der Laan
Magnetic Spectroscopy, Daresbury Laboratory, Warrington WA4 4AD, United Kingdom
(Received 23 July 2002; published 23 October 2002)

We present calculations for the magnetic circular dichroism (MCD) in the $3d^n \rightarrow 2p^5 3d^{n+1} \rightarrow 3p^4 3d^{n+1}\varepsilon$ photoemission process in resonance with the $2p$ x-ray absorption from ferromagnetic Ni in perpendicular geometry (PG). The calculations are based on a coherent second-order optical process taking into account the intra-atomic multiplet and the configuration interaction. The MCD in PG at the L_3 edge is found to be in excellent agreement with the previous experimental results. At the excitation energy of the 4-eV and 6-eV satellites, the predicted MCD is strongly different, which should permit to assess the angular dependence of the intra-atomic Coulomb interaction.

DOI: 10.1103/PhysRevB.66.140401 PACS number(s): 75.25.+z, 78.20.Ls, 78.70.Dm, 79.60.−i

X-ray-absorption spectroscopy (XAS) using circularly polarized radiation, which gives rise to magnetic circular dichroism (MCD), has proven to be ideal to study the local electronic and magnetic properties of materials since the relevant ground-state properties can be determined using powerful sum rules.[1–3] It is well known that the MCD in XAS (MCD-XAS) vanishes when the helicity vector of the incident light is perpendicular to the remanent magnetization direction. However, in this perpendicular geometry (PG) the MCD can still be present in the decay process (see Fig. 1). Thole, Dürr, and van der Laan[4] reported MCD in resonant photoemission (MCD-RPE) of 9% in the $2p3p3p$ decay from ferromagnetic Ni measured in PG. This effect was also observed in the Ni $2p3d3d$ and Fe $2p3p3p$ decays.[5,6] It was also unexpectedly found in the Fe $L_3M_{2,3}M_{2,3}$ Auger spectral of ferromagnetic Fe (using a photon energy of 900 eV). A qualitative explanation for the effect in Auger spectral which is absent in ferromagnet Mn and Ni,[7] was given in Ref. 8. Braicovich *et al.*[9] observed that also the MCD in resonant x-ray Raman scattering (MCD-RXRS) does not vanish in PG. These measurements show which MCD-RPE and MCD-RXRS can provide information about the core-hole polarization that is not accessible by MCD-XAS.

To our knowledge, only two theoretical calculations in PG have been performed so far. The MCD in the Ni $2p3p3p$ RPE decay was calculated for the atomic process $3d^9 \rightarrow 2p^5 3d^{10} \leftrightarrow 3p^4 3d^{10}\varepsilon \leftrightarrow 3s^1 3d^9 \varepsilon$, where ε denotes a continuum photoelectron.[10] Recently, also Fukui *et al.*[11] showed for Gd $4f^7$ that the atomic calculation of MCD-RXRS for the $2p \rightarrow 5d$ excitation followed by $3d \rightarrow 2p$ radiative decay is in good agreement with experiments on $Gd_{33}Co_{67}$ amorphous alloy. They claimed that the MCD-RXRS in PG is caused by cross terms, that are characteristic of the coherent second-order optical process. However, it was already shown by van der Laan and Thole[10] that a two-step model is also able to explain the MCD in PG. There are a few further questions that need to be addressed by detailed calculations and for which the Ni $2p3p3p$ decay can be considered as archetypal, namely,

(i) *Core-hole interaction:* Using the two-step model, it was shown that for Ni $3d^9$ the shape of the MCD-RPE is independent of the emission angle.[10] However, the general formula for second-order processes shows that in the presence of core-valence interactions the two-step model may break down due to interference terms between intermediate states separated by more than their lifetime width.

(ii) *Final-state interference:* This arises due to the decay to different photoemission continua. In the $3p^4$ final state, interference occurs only for the ^1D level, which is part of the negative lobe of the MCD (see Fig. 2). It was already shown that its MCD signal is sensitive to the phase factor of the outgoing photoelectron wave functions.[6]

(iii) *Integrated intensity:* For both Fe and Ni the experimental MCD is ~ 3 times smaller than theoretically predicted. Using the sum rules this would suggest that the actual

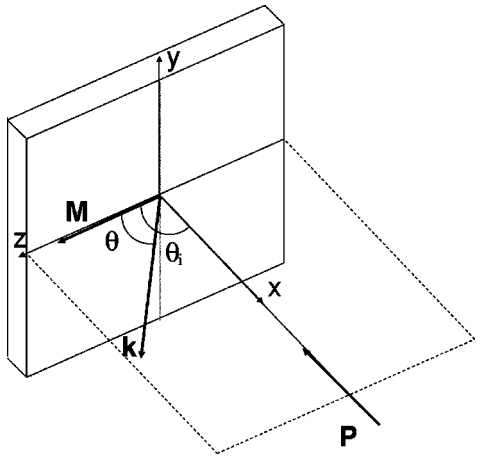

FIG. 1. Perpendicular geometry (PG) for RPE, where **P**, **M**, and **k** are the helicity vector of the incident circularly polarized x rays, the remanent magnetization direction, and the detection direction of the emitted photoelectrons, respectively. **P** and **k** have angles θ_i and θ, respectively, with **M**. Reversal of either **M** or **P** results in a different geometry. Since **k** is even, reversal of both **M** or **P** together renders the same geometry, hence the condition for MCD is satisfied.

 ©2002 The American Physical Society

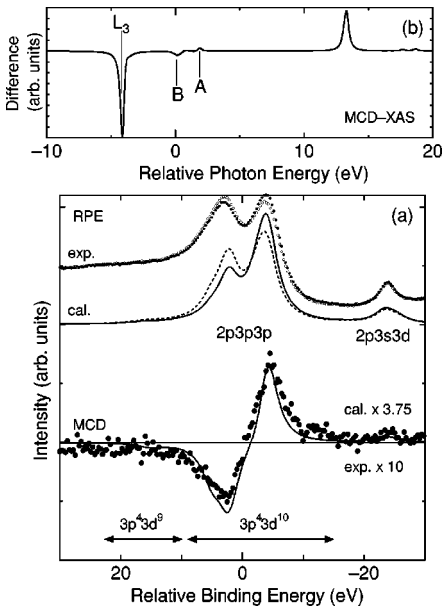

FIG. 2. (a) Calculated Ni $2p3p3p$ and $2p3s3d$ RPE from ferromagnetic Ni in PG with photon energy at the L_3 and its MCD for positive (dashed line) and negative (solid line) helicity incident light, and compared to the experimental results (dots) taken from Ref. 4. (b) Calculated Ni $L_{2,3}$ MCD-XAS.

ground-state polarization is smaller than expected.[6] In order to verify the earlier predictions and to shed new light on the above-mentioned questions, we extended the radiative transition-probability code for the Anderson impurity model to include angle dependent resonant photoemission. So far, these calculations were done for the angle-integrated case only.[12,13]

The experimental $2p$ XAS of Ni metal shows satellites at 4 and 6 eV above the L_3 edge.[14] Several theoretical models have been proposed but the interpretation remains controversial. One-electron band theory assigns the 6-eV satellite to a van-Hove singularity at the L point,[15] but fails to explain the prominent 4-eV satellite in MCD-XAS.[14] The periodic four-site cluster model, which takes into account the band dispersion, gives a good agreement with the experimental valence band[16] and $2p$ photoemission,[17] but resulted in an incorrect $2p$ MCD-XAS.[18] A suitable alternative is the configuration-interaction (CI) model based on the localized Anderson impurity approach with the multiplet interaction,[12,19,20] which shows a good agreement for a wide variety of core-level spectroscopies.[21] The CI model reproduces the $2p$ satellites as a predominantly $2p^5 3d^9$ final state with an energy splitting due to the $2p$-$3d$ exchange interaction [Fig. 2(b)].

In the calculation,[12,19,20] we select a central Ni atom with appropriate linear combinations of $3d$ orbitals on neighboring sites to serve as a reservoir of holes that are denoted by $\underline{L}$. The Hamiltonian contains three terms H_0+T+R. The H_0 describes the localized Anderson impurity model including intra-atomic multiplet interaction and interatomic hybridization V. The electric-dipole transition operator T leads to $2p \rightarrow 3d$ XAS. The Coulomb interaction $R(2p,3p;3p,\varepsilon)$ is responsible for the photoemission decay. The coherent second-order process can be represented by

$$
\begin{array}{ccccccccc}
 & & 3d^{10}\underline{L}^2 & & & & & & \\
 & & \updownarrow & & & & & & \\
3d^9\underline{L} & \overset{T}{\rightarrow} & 2p^5 3d^{10}\underline{L} & \overset{R}{\rightarrow} & 3p^4 3d^{10}\underline{L}\varepsilon & \leftrightarrow & 3s^1 3d^9\underline{L}\varepsilon & & \text{(I)} \\
 & & \updownarrow & & & & & & \\
3d^8 & \overset{T}{\rightarrow} & 2p^5 3d^9 & \overset{R}{\rightarrow} & 3p^4 3d^9\varepsilon & \leftrightarrow & 3s^1 3d^8\varepsilon & & \text{(II)}
\end{array}
$$

where the ground state $|g\rangle$, intermediate state $|m\rangle$, and final state $|k\beta\rangle=|k\rangle|\beta\rangle$ are a mixture of the configurations $3d^n$, $2p^5 3d^{n+1}$, and $3p^4 3d^{n+1}\varepsilon$, respectively, with energies E_g, E_m, and $E_{k\beta}=\varepsilon_k+E_\beta$, respectively, where $|k\rangle$ and ε_k represent the continuum photoelectron state and its energy. The direct photoemission channel $2p^5 3d^{n+1} \rightarrow 3s^1 3d^n$ was also included. The two-core-hole final state $3p^4 3d^{n+1}$ cannot be reached by direct photoemission and has CI with $3s^1 3d^n$.[12]

In the discussion that follows, we will refer to the pathways I and II of this process. Strictly speaking, unless $V \rightarrow 0$, these pathways cannot be separated, since at each stage of the process the configurations are mixed due to hybridization.

The spectral function of the RPE is

$$
F(h\nu,E)=\sum_{k,\beta}\left|\sum_m \frac{\langle k\beta|R|m\rangle\langle m|T|g\rangle}{E_g+h\nu-E_m-i\Gamma_M}\right|^2 \times \delta(h\nu+E_g-E_{k\beta})\,\delta(E-\varepsilon_k), \qquad (1)
$$

where $h\nu$ is the incident photon energy, E is the photoelectron energy, and Γ_M is the broadening of the intermediate state due to the core-hole lifetime.

The wave function of the ejected photoemission electron in the continuum state traveling with energy ε_k indirection $\hat{k}$ is given by a superposition of an outgoing plane wave and incoming spherical waves,[22]

$$
|\mathbf{k}\rangle=\frac{1}{k}\sum_{l,m} i^l e^{-i\delta_l} Y_{lm}^*(\hat{k}) R_{\varepsilon_k l}(r) Y_{lm}(\hat{r}), \qquad (2)
$$

where δ_l is the total phase shift of the lth partial wave and $R_{\varepsilon_k l}(r)$ is the radial part, and the spherical harmonics Y_{lm} have the usual phase convention.[23] Substitution of Eq. (2) into Eq. (1) can lead to interference between spherical harmonics with different l values. The angle dependent MCD spectrum can be sensitive to the phase factor of the photoelectron. The specific choice of the outgoing wave can be important. For instance, a wave function represented by spherical harmonics corresponds to Eq. (5) without the factor i^l, and would give a different MCD for the $3p^4\ ^1D$ level.[10] In the case of angle integrated MCD, the phase factor of the ejected photoelectron, $i^l e^{-i\delta_l} Y^*_{lm}(\hat{k})$, can be omitted. This is, e.g., supported by the MCD-RPE calculations for Tb, which are in good agreements with experimental results.[13]

Using the coordinates of Fig. 1, the MCD-RPE is

$$\Delta F \equiv F_- - F_+ = \sum_{k,\beta} \left\{ \cos\theta_i (|f_{-1}|^2 - |f_1|^2) - \frac{\sin\theta_i}{\sqrt{2}} (f_1 f_0^* + f_{-1} f_0^* + f_0 f_1^* + f_0 f_{-1}^*) \right\}, \quad (3)$$

$$f_q(\theta) \equiv \sum_m \frac{\langle k\beta|R|m\rangle\langle m|T_q|g\rangle}{E_g + h\nu - E_m - i\Gamma_M}, \quad (4)$$

where T_q is the electric-dipole operator with polarization $q = \pm 1,0$. Equation (3) holds for RPE and by replacing the f_q's we obtain the equivalent for RXRS, i.e., Eq. (2) in Ref. 11.

The spectral function ΔF in Eq. (3) consists of two terms. The first term contains the diagonal terms $|f_q|^2$, while the second one contains the cross terms caused by the interference effects in the intermediate state of the coherent second-order optical process. In parallel geometry ($\theta_i = 0°$), the cross terms vanish and only the diagonal terms remain. In PG ($\theta_i = 90°$) the diagonal terms vanish and only the cross terms remain. Both terms are sensitive to the final-state interference due to Eq. (2), but this effect is much more pronounced in PG.

We will now discuss the calculated results of the Ni $2p3p3p$ decay in PG. The parameters can be found elsewhere and have been scaled to fit the experiment Ref. 24. The RPE and MCD spectra are shown in Fig. 2(a) for $\theta = 60°$, and $\theta_i = 90°$ and with $h\nu$ tuned to the maximum of the L_3 MCD-XAS. The RPE consists of a double peak of mainly $3p^4 3d^{10}$ character dwarfing a weak satellite structure of mainly $3p^4 3d^9$ character at higher binding energy. Due to the strong CI with the $3s^1 3d^9$, there is also MCD in the $2p3s3d$ decay, which is at lower binding energy. Figure 2(a) shows that the shape of the calculated MCD is in excellent agreement with the experiment but ~ 3 times larger, which confirms the value obtained in Ref. 4.

Figure 3 shows that when $h\nu$ is tuned to the energy of satellites A and B, the $3p^4 3d^9$ is strongly enhanced. This can be understood by realizing that at the L_3 maximum the process is dominated by pathway I, but pathway II becomes more important at higher photon energies. For $h\nu = A$, the relative weight of the $2p^5 3d^9$ is higher than for $h\nu = B$, resulting in an increased intensity for the $3p^4 3d^9$. Furthermore, the shape of the MCD spectra is quite different at both photon energies. Although the shape is complicated, its origin is revealed by separating the different $3p^4 3d^{n+1}$ contributions to the final state. Figure 3 shows that the MCD of the $3p^4 3d^{10}$ contribution has a similar shape for A and B and resembles that of the L_3. Also the $3p^4 3d^9$ displays a similar spectral shape for A and B, however, in this case the sign is reversed. This might be interesting to verify experimentally, although one should keep in mind that in the measurement at photon energies above the edge, the RPE also interferes with Auger emission such as $3d^n \rightarrow 2p^5 3d^n \varepsilon \rightarrow 3p^4 3d^9 \varepsilon\varepsilon'$, which was not included in our calculation.

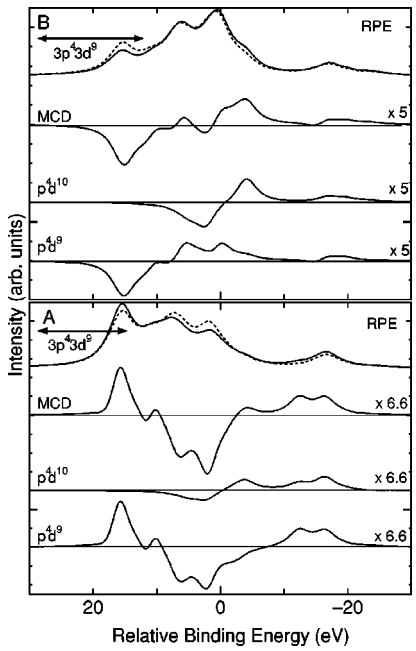

FIG. 3. Calculated Ni $2p3p3p$ and $2p3s3d$ RPE and its MCD in PG from ferromagnetic Ni with the photon energy at the satellites A and B of the MCD-XAS in Fig. 2(b) for $\theta = 60°$ and $\theta_i = 90°$. The two separate contributions arising from the $3p^4 3d^9$ and $3p^4 3d^{10}$ in the MCD-RPE spectra are also shown.

It is also of interest to consider the angular dependence of the emitted photoelectron for different $h\nu$. The calculated results are presented in Fig. 4. For all photon energies, the MCD vanishes at 0° and 90°. The inset shows the θ dependence at the L_3 for x rays with negative helicity. The RPE itself is θ dependent but its spectral shape is not. This behavior has been explained in Ref. 10 using the fundamental spectra analysis under the assumption that pathway I prevails for the L_3. This model neglects the angular dependence of the $2p$-$3d$ Coulomb interactions and therefore it holds for pathway, I but not necessarily for pathway II. Equation (58) of Ref. 10 gives the $2p3p3p$ MCD-RPE as a linear combination of two fundamental spectra B^0 and B^2. The angular coefficient for the B^0 spectrum is $\cos\theta_i$. This vanishes in PG, so that the MCD-RPE becomes equal to the B^2 spectra ($\times \frac{1}{2}\sin 2\theta$). Thus the spectral shape of the MCD is conserved

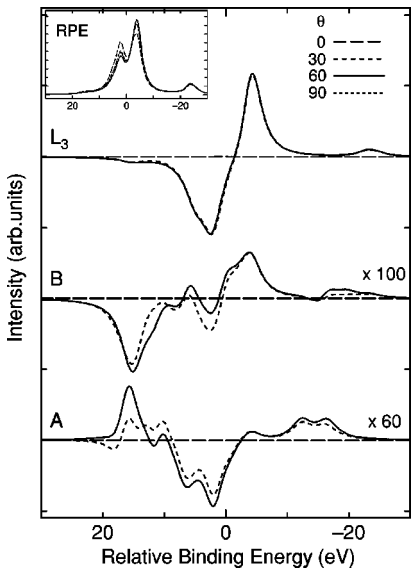

FIG. 4. Calculated results showing the angular dependence of the MCD-RPE in PG. The inset shows the angle-dependent RPE at the L_3 energy for incident photons with negative helicity vector.

and only the total intensity depends on θ. This simple proof also demonstrates the strength of the fundamental-spectra analysis compared to, e.g., the method of Eq. (3) where the angular dependence is a function of $h\nu$ and E_B.

Figure 4 shows that for $h\nu$ equal to *A* or *B*, the MCD-RPE spectrum depends strongly on θ. It is seen that the change in the $3p^4 3d^9$ is much larger than in the $3p^4 3d^{10}$ region, because of the pathway assumption in the approach of Ref. 10. This indicates that the influence of the angle-dependent $2p$-$3d$ Coulomb interactions can be studied with MCD-RPE.

In summary, the $2p3p3p$ MCD-RPE from ferromagnetic Ni in PG has been calculated using the full CI model. The shape of the calculated spectrum at the L_3 edge is in excellent agreement with the experimental results, indicating the importance of the phase factor of the ejected photoelectron in the angular dependence. However, it is confirmed that the experimental value of the MCD is ~ 3 times smaller than the theoretical calculation. We have verified that for a ground state $3d^9$ the two-step model gives the same results as the coherent second-order optical process. The predicted MCD-RPE spectra at the satellite energies show a significant angular dependence that would be interesting to verify experimentally since it could provide information about the angular dependence of the core-valence Coulomb interaction.

M.T. is grateful to H. Ogasawara and T. Uozumi for valuable discussions.

[1] B.T. Thole *et al.* Phys. Rev. Lett. **68**, 1943 (1992).
[2] P. Carra *et al.*, Phys. Rev. Lett. **70**, 694 (1993).
[3] G. van der Laan, Phys. Rev. B **57**, 112 (1998).
[4] B.T. Thole *et al.*, Phys. Rev. Lett. **74**, 2371 (1995).
[5] H.A. Dürr *et al.*, J. Phys.: Condens. Matter **8**, L7 (1996).
[6] G. van der Laan, H.A. Dürr, and M. Surman, J. Electron Spectrosc. Relat. Phenom. **78**, 213 (1996).
[7] H.A. Dürr *et al.*, Europhys. Lett. **40**, 171 (1997).
[8] H.A. Dürr *et al.*, J. Electron Spectrosc. Relat. Phenom. **93**, 233 (1998).
[9] L. Braicovich *et al.*, Phys. Rev. Lett. **82**, 1566 (1999).
[10] G. van der Laan and B.T. Thole, J. Phys.: Condens. Matter **7**, 9947 (1995).
[11] K. Fukui *et al.*, J. Phys. Soc. Jpn. **70**, 1230 (2001).
[12] G. van der Laan *et al.* Phys. Rev. B **46**, 9336 (1992).
[13] G. van der Laan *et al.*, Phys. Rev. B **59**, 8835 (1999).
[14] C.T. Chen *et al.*, Phys. Rev. B **42**, 7262 (1990).
[15] H. Ebert, Rep. Prog. Phys. **59**, 1665 (1996).
[16] R.H. Victora and L.M. Falicov, Phys. Rev. Lett. **55**, 1140 (1985).
[17] J.G. Menchero, Phys. Rev. Lett. **76**, 3208 (1996).
[18] N. Manini *et al.*, Phys. Rev. Lett. **79**, 2594 (1997).
[19] T. Jo and G.A. Sawatzky, Phys. Rev. B **43**, 8771 (1991).
[20] G. van der Laan and B.T. Thole, J. Phys.: Condens. Matter **4**, 4181 (1992).
[21] G. van der Laan *et al.*, Phys. Rev. B **61**, 12 277 (2000), and references therein.
[22] G. Breit and H.A. Bethe, Phys. Rev. **93**, 888 (1954).
[23] E. U. Condon and G. H. Shortley, *The Theory of Atomic Spectra* (Cambridge University Press, Cambridge, 1959).
[24] If we denote the charge-transfer energy from the reservoir to the $3d$ states as $\Delta \equiv \epsilon_d - \epsilon_v + 9U$, the difference between the configuration-averaged energies, in the limit of $V \to 0$, is $E(d^9\underline{L}) - E(d^8) = \Delta - U$ and $E(d^{10}\underline{L}^2) - E(d^8) = 2\Delta - U$, where U is the on-site $3d$ Coulomb interaction. For the ground state, we used similar parameters as in Ref. 20, namely $\Delta = -0.75$, $V(e_g) = -2V(t_{2g}) = 1.6$, and $U = 1.5$ eV, with the difference that we used O_h instead of D_{3d} symmetry to reduce the size of the calculation. The $^3A_1$ ground state has 14.9% $3d^8$, 48.7% $3d^9$, and 36.4% $3d^{10}$ character. The core-valence Coulomb interactions are $U_{2p3d} = 2.5$ and $U_{3p3d} = 4.5$ eV. The lifetime broadening of the $2p$ core hole, Γ_M, is taken as 0.2 eV HWHM and that of the $3s$ and $3p$ core-hole Γ_L as 2.0 eV (HWHM). We adopt the Slater integrals, Coulomb matrix elements values, and photoelectron phase difference $\delta_f - \delta_p$ as in Refs. 10,12. All Slater integrals are reduced to 80%. The radial matrix elements $R(2p3p;3p\varepsilon l)$ are reduced to 75% of the Hartree-Fock values. The average energy difference between the $3p^4 3d^{n+1}$ and $3s^1 3d^n$ configurations was calculated using Cowan (Ref. 25): $E_{av}(3p^4 3d^9) - E_{av}(3s^1 3d^8) = 26.448$ eV, $E_{av}(3p^4 3d^{10}) - E_{av}(3s^1 3d^9) = 26.745$ eV. These values are scaled down to 85% to fit the experiments.
[25] R. D. Cowan, *The Theory of Atomic Structure and Spectra* (University of California Press, Berkeley, 1981).